



Ultrasonographic Diagnosis of Biliary Atresia Based on a Decision-Making Tree Model

So Mi Lee, MD, Jung-Eun Cheon, MD, Young Hun Choi, MD, Woo Sun Kim, MD, Hyun-Hye Cho, MD, In-One Kim, MD, Sun Kyoung You, MD

All authors: Department of Radiology, Seoul National University College of Medicine, Seoul 03080, Korea

Objective: To assess the diagnostic value of various ultrasound (US) findings and to make a decision-tree model for US diagnosis of biliary atresia (BA).

Materials and Methods: From March 2008 to January 2014, the following US findings were retrospectively evaluated in 100 infants with cholestatic jaundice (BA, n = 46; non-BA, n = 54): length and morphology of the gallbladder, triangular cord thickness, hepatic artery and portal vein diameters, and visualization of the common bile duct. Logistic regression analyses were performed to determine the features that would be useful in predicting BA. Conditional inference tree analysis was used to generate a decision-making tree for classifying patients into the BA or non-BA groups.

Results: Multivariate logistic regression analysis showed that abnormal gallbladder morphology and greater triangular cord thickness were significant predictors of BA ($p = 0.003$ and 0.001 ; adjusted odds ratio: 345.6 and 65.6, respectively). In the decision-making tree using conditional inference tree analysis, gallbladder morphology and triangular cord thickness (optimal cutoff value of triangular cord thickness, 3.4 mm) were also selected as significant discriminators for differential diagnosis of BA, and gallbladder morphology was the first discriminator. The diagnostic performance of the decision-making tree was excellent, with sensitivity of 100% (46/46), specificity of 94.4% (51/54), and overall accuracy of 97% (97/100).

Conclusion: Abnormal gallbladder morphology and greater triangular cord thickness (> 3.4 mm) were the most useful predictors of BA on US. We suggest that the gallbladder morphology should be evaluated first and that triangular cord thickness should be evaluated subsequently in cases with normal gallbladder morphology.

Index terms: Neonatal jaundice; Biliary atresia; US; Decision trees

INTRODUCTION

Biliary atresia (BA) is a progressive fibro-obliterative

Received January 13, 2015; accepted after revision September 19, 2015.

Corresponding author: Jung-Eun Cheon, MD, Department of Radiology and Institute of Radiation Medicine, Seoul National University College of Medicine, 101 Daehak-ro, Jongno-gu, Seoul 03080, Korea.

• Tel: (822) 2072-3608 • Fax: (822) 747-5781
• E-mail: cheonje@snu.ac.kr

This is an Open Access article distributed under the terms of the Creative Commons Attribution Non-Commercial License (<http://creativecommons.org/licenses/by-nc/3.0>) which permits unrestricted non-commercial use, distribution, and reproduction in any medium, provided the original work is properly cited.

process of the bile duct (1) that leads to early biliary cirrhosis. An early and accurate preoperative diagnosis of BA is required because the Kasai operation has been shown to be more successful when performed within 90 days of birth (2). Therefore, it is important to differentiate BA from other medically treatable causes of cholestatic jaundice. However, making a definitive diagnosis preoperatively is challenging owing to the considerable clinical, histopathologic, and radiologic overlap that exists between BA and other cause of cholestatic jaundice (1, 3-5).

Ultrasound (US) has been playing an important role in screening for infantile cholestasis. A number of US findings have been described as useful predictors of BA (4, 6-12). Atretic gallbladder (6) and triangular cord sign

(4, 7-9) have been shown to be useful indicators with variable diagnostic performances. In addition, other US findings such as visualization of extrahepatic bile duct (11), diameter of the hepatic artery (12), and presence of hepatic subcapsular flow (13, 14) have been evaluated. However, in clinical situations, we usually make the US diagnosis of BA considering all of these findings rather than depending on a single US finding. Moreover, it is sometimes difficult to decide which US findings we should prioritize, especially in the conflicting cases. Therefore, a more staged approach using a decision-making tree-based on the assessments of priorities on the aforementioned US findings—is necessary for evaluating infants with cholestatic jaundice. Thus, a conditional inference tree analysis was adapted to generate a decision-making tree. Conditional inference trees, a predictive modeling approach, evaluate a regression relationship by binary recursive partitioning in a conditional inference framework. This statistics-based approach automatically selects the input variable with strongest association with the outcome and performs a binary split in the selected input variable. These two steps are recursively repeated, thereby creating a decision tree—a flow-chart-like structure—that predicts outcomes (15).

The present study aimed to assess the diagnostic value of various US findings and to establish a US decision-making tree model for the differential diagnosis of BA from other causes of cholestasis.

MATERIALS AND METHODS

Patients

Our Institutional Review Board approved the present study and waived the requirements for informed consent. This retrospective study was based on data collected from March 2008 to January 2014. US was performed in 171 consecutive neonates and infants with persistent jaundice. Seventy-one of the 171 patients were excluded from the study owing to unconjugated jaundice related to breast milk feeding or prematurity ($n = 43$), choledochal cyst ($n = 4$), and loss to follow-up ($n = 24$). Data on the total serum bilirubin (normal: 0.2–1.2 mg/dL), direct bilirubin (normal: 0–0.5 mg/dL), and γ -glutamyl transferase (normal: 8–35 IU/L) levels at the time of admission were obtained by reviewing medical charts. The diagnosis of BA was confirmed by means of Kasai surgery and the intraoperative cholangiographic findings, as well as histologic findings of the specimen that revealed the fibrotic obstruction of the extrahepatic

biliary duct. The absence of BA was determined based on clinical improvement during the follow-up period (evidenced by clinical improvement of jaundice and normalization of laboratory results) ($n = 46$), pathologic findings of a liver biopsy specimen ($n = 21$), radioisotope biliary excretion scan ($n = 25$), normal intraoperative cholangiographic findings (showing a patent biliary system) ($n = 3$), or a genetic study ($n = 6$). Finally, 100 patients (male-to-female ratio, 51:49; mean age, 55 days; age range, 3–129 days) with or without diagnosed BA were enrolled in our study.

US Image Analysis

All 100 patients were scanned by one of the 3 pediatric radiologists (with 25, 16, and 10 years of experience with pediatric US, respectively) on an iU22 (Philips, Bothell, WA, USA) with 4–9 MHz convex and 5–12 MHz linear transducers, a Sequoia 512 (Acuson, Mountain View, CA, USA) with 2–6 MHz convex and 8–15 MHz linear transducers, or an Aplio XG (Toshiba, Tokyo, Japan) with 3.6–9.2 MHz convex and 8–14 MHz linear transducers. The patients were fasted for ≥ 4 hours before the examination and not sedated. The US findings were retrospectively reviewed in consensus by 2 radiologists (with 10 and 6 years of experience, respectively) at the picture archiving and communication system workstation (Maroview; Marotech, Seoul, Korea). High-frequency transducers (> 10 MHz) were used to evaluate the gallbladders. Gallbladder length was measured along the long axis. Gallbladder morphology was classified into two types (16–18). Abnormal gallbladder was defined as follows: 1) nonvisualization of gallbladder; 2) gallbladder detected with atretic lumen and lumen length equal or less than 15 mm; 3) gallbladder detected with distended lumen and lumen length more than 15 mm but lack of complete mucosal lining or uneven echogenic outer wall thickness with irregular shape. Normal gallbladder was defined as follows: 1) gallbladder detected with fully distended lumen and lumen length more than 15 mm and smooth and complete mucosal lining with uniformly thin wall; or 2) gallbladder detected with collapsed or partially filled lumen but smooth and complete mucosal lining and uniformly thickened wall seen as a hypoechoic layer between the inner and outer walls. Triangular cord was defined as a thick tubular or triangular echogenic density along the anterior aspect of the portal vein (9). The thickness of the triangular cord was measured at the porta hepatis on the oblique longitudinal or transverse scans. The diameter of the hepatic artery was measured at the level of

the right proximal hepatic artery, which runs parallel to the right portal vein, and the diameter of the portal vein was measured at the right proximal portal vein, just proximal to the division of the anterior and posterior branches. The measurement was made by using an electronic caliper from the mid-portion of the anterior wall to the mid-portion of the posterior wall of the hepatic artery and portal vein. Moreover, we also assessed whether the common bile duct (CBD) was visible. When required, color Doppler scan was used to help identify the CBD. Hepatic subcapsular flow was not included in the US image analysis because it was not evaluated in most of our cases.

Statistical Analysis

The *t* test was used to compare the age and laboratory findings between the BA and non-BA groups. The Pearson's χ^2 test was used to compare the male-to-female ratios between the two groups. Receiver operating characteristic (ROC) curves were constructed to evaluate the diagnostic performance of the laboratory findings. Univariate logistic regression analysis was performed to identify the US findings that could predict BA. Multivariate logistic regression analysis using the backward elimination method was subsequently performed to identify the significant independent predictors of BA. The significant US findings with a *p* value of < 0.1 in the univariate analysis were included in the multivariate analysis. A *p* value of < 0.05 was considered statistically significant, and the data analyses were performed with commercially available statistical software (SPSS, version 12; SPSS Inc., Chicago, IL, USA). Conditional inference tree analysis was performed to determine the US findings with the strongest associations with BA and to generate a decision-making tree for classifying patients into the BA or non-BA groups using the statistical software package R (R for Windows, version 2.10.0; R development Core Team, Vienna, Austria, <http://www.R-project.org>) (Appendix E1 in the online-only Data Supplement for further description of the conditional inference tree analysis).

RESULTS

Clinical Findings

Biliary atresia was surgically confirmed in 46 patients (mean age, 60 days; range, 11–124 days; male-to-female ratio, 21:25). The remaining 54 patients (mean age, 51 days; range, 3–129 days; male-to-female ratio, 30:24) were

assigned to the non-BA group: idiopathic neonatal hepatitis (n = 38), progressive familial intrahepatic cholestasis (PFIC) (n = 4), total parenteral nutrition associated cholestasis (n = 3), Alagille syndrome (n = 4), cytomegalovirus hepatitis (n = 2), fetal alcoholic syndrome (n = 1) and neonatal intrahepatic cholestasis caused by citrin deficiency (NICCD) (n = 2). Neonatal hepatitis was confirmed with clinical improvement (n = 31) or percutaneous needle biopsy (n = 7). PFIC was confirmed with ABCB11 mutation (n = 1) or immunohistochemical staining and electron microscopy of liver specimen (n = 3). Alagille syndrome was confirmed with clinical criteria and percutaneous liver biopsy (n = 1) or mutation in the JAG 1 gene (n = 3). NICCD was confirmed with mutation in the SLC25A13 gene.

Clinical characteristics between the BA and non-BA groups showed no significant differences in age (*p* = 0.106), male-to-female ratio (*p* = 0.323), or total serum bilirubin between the groups (*p* = 0.193); however, a statistically significant difference was observed in the direct bilirubin levels (*p* = 0.028), and γ -glutamyl transferase levels (*p* < 0.001) (Table 1). According to ROC curve analysis, the optimal cutoff values of direct bilirubin and γ -glutamyl transferase levels were 5 mg/dL and 200 IU/L, respectively. Area under the ROC curve, sensitivity, specificity, positive predictive value, and negative predictive value of direct bilirubin and γ -glutamyl transferase levels in the identification of BA are listed in Table 2.

Analysis of the US Imaging

In the univariate analysis, BA was significantly associated with the following US findings: abnormal gallbladder morphology (*p* < 0.001), shorter gallbladder length (*p* < 0.001), higher triangular cord thickness (*p* < 0.001), greater hepatic artery diameter (*p* < 0.001), greater portal vein diameter (*p* = 0.012), and non-visualization of the CBD (*p* = 0.001). The multivariate logistic analysis showed that abnormal gallbladder morphology (odds ratio = 345.63, *p* = 0.003) and greater triangular cord thickness (odds ratio = 65.64, *p* = 0.001) were the only 2 findings that were independently associated with BA. The summary of the US findings in the BA and non-BA groups and the results of the logistic regression analysis to identify predictors of BA are presented in Table 3.

Conditional Inference Tree Analysis

In the conditional inference tree analysis, the two US findings (gallbladder morphology and triangular cord

Table 1. Clinical Findings at Time of US Examinations

Variables	BA (n = 46)	Non-BA (n = 54)	P
Age (day)	60 ± 21 (11–124)	51 ± 29 (3–129)	0.106
Male-to-female ratio	21:25	30:24	0.323
Total bilirubin (mg/dL)	10.4 ± 4.5 (3.3–29.4)	11.8 ± 5.8 (3–30.8)	0.193
Direct bilirubin (mg/dL)	6.7 ± 2.6 (2.1–13.9)	5.4 ± 3.1 (0.8–15.4)	0.028
GGT (IU/L)	516 ± 386.6 (74–1850)	193 ± 213.5 (30–1138)	< 0.001

Unless otherwise indicated, data are means ± standard deviations, with ranges in parentheses. BA = biliary atresia, GGT = γ -glutamyl transferase, US = ultrasound

Table 2. Diagnostic Performance of Laboratory Findings in Diagnosis of BA

Laboratory Parameters	AUC*	Optimal Cutoff Value	Sensitivity [†]	Specificity [†]	PPV [†]	NPV [†]
Direct bilirubin (mg/dL)	0.677 (0.576–0.767)	5	73.9 (34/46)	61.1 (33/54)	61.8 (34/55)	84.6 (33/39)
GGT (IU/L)	0.848 (0.761–0.914)	200	86.9 (40/46)	76 (38/50)	76.9 (40/52)	86.4 (38/44)

*Numbers in parentheses are 95% confidence intervals, [†]Data are percentages, with numbers of patients in parentheses. AUC = areas under the receiver operating characteristic curve, BA = biliary atresia, GGT = γ -glutamyl transferase, NPV = negative predictive value, PPV = positive predictive value

Table 3. Comparison of US Parameters

Findings	BA (n = 46)	Non-BA (n = 54)	Univariate		Multivariate	
			OR (95% CI)	P	OR (95% CI)	P
Gallbladder morphology [†]			94.71 (23.00–390.02)	< 0.001	345.63 (7.58–15762.12)	0.003
Normal	7 (15)	51 (94)				
Abnormal	39 (85)	3 (6)				
Gallbladder length (mm) [‡]	14.3 ± 6.4 (0–25.7)*	22.4 ± 5.91 (0–36.5)*	0.82 (0.75–0.89)	< 0.001		
Triangular cord thickness (mm) [‡]	4.1 ± 0.9 (2.2–6.8)	2.2 ± 0.5 (1–3.4)	90.78 (12.68–646.92)	< 0.001	65.64 (5.31–811.67)	0.001
Diameter of HA (mm) [‡]	1.8 ± 0.4 (1–3)	1.2 ± 0.2 (0.8–1.7)	2956.32 (136.60–63979.94)	< 0.001		
Diameter of PV (mm) [‡]	3.8 ± 0.8 (2–5.6)	3.4 ± 0.7 (1.5–5.2)	2.09 (1.18–3.71)	0.012		
CBD [†]			0.11 (0.03–0.40)	0.001		
Detected	3 (7)	21 (39)				
Undetected	43 (93)	33 (61)				

Variables showing *p* value of less than 0.1 in univariate analysis were included in multivariate analysis. *Gallbladders were not visualized in 3 patient with BA and 1 patient with non-BA, [†]Data are numbers of patients, with percentages in parentheses, [‡]Data are mean values ± standard deviations, with ranges in parentheses. BA = biliary atresia, CBD = common bile duct, CI = confidence interval, HA = hepatic artery, OR = odds ratio, PV = portal vein, US = ultrasound

thickness) were identified as significant predictors of the presence or absence of BA (*p* < 0.001) (Fig. 1). The first split of the tree was made according to the gallbladder morphology. Abnormal gallbladder morphology—regardless of triangular cord thickness—led to node 5, which had 39 (92.9%) patients with BA and 3 (7.1%) patients without BA (Figs. 2, 3). In the other branch, which showed normal gallbladder morphology, the next division was based on

the triangular cord thickness. The optimal cutoff value of triangular cord thickness for a diagnosis of BA was automatically selected as 3.4 mm by the statistical method. Normal gallbladder morphology with triangular cord thickness > 3.4 mm led to node 4. All 7 cases in node 4 had BA (Fig. 4). The remaining 51 cases with normal gallbladder morphology and triangular cord thickness ≤ 3.4 mm reached node 3, in which no patients had BA.

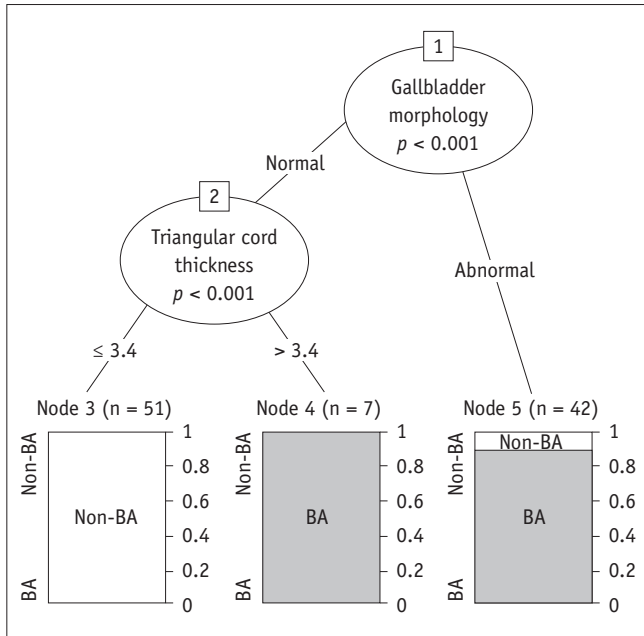


Fig. 1. Conditional inference tree for diagnosis of BA. For each inner node (nodes 1 and 2), gallbladder morphology and triangular cord thickness were selected (p value, < 0.001), and percentage of BA is shown for each terminal node (node 3–5). First split of tree was made according to gallbladder morphology. Abnormal morphology—regardless of triangular cord thickness—led to node 5, which had 39 (92.9%) patients with BA and 3 (7.1%) patients without. In other branch, which showed normal gallbladder morphology, next division was based on triangular cord thickness. Optimal cutoff value of triangular cord thickness for diagnosis of BA was automatically selected as 3.4 mm. Normal gallbladder morphology with triangular cord thickness > 3.4 mm led to node 4, and all 7 cases (100%) in node 4 had BA. Normal gallbladder morphology with triangular cord thickness ≤ 3.4 mm reached node 3, in which none of 51 patients (100%) had BA. BA = biliary atresia

Diagnostic Performance of US Findings

When these criteria—abnormal gallbladder morphology regardless of triangular cord thickness (node 5) or triangular cord thickness > 3.4 mm despite normal gallbladder morphology (node 4)—were applied according to the results of the conditional inference tree in the diagnosis of BA, the following results were obtained: a sensitivity of 100% (46 of 46), a specificity of 94.4% (51 of 54), a positive predictive value of 93.9% (46 of 49), a negative predictive value of 100% (51 of 51), and an overall accuracy of 97% (97 of 100). There were no false-negatives and 3 false-positive cases. These 3 patients showed abnormal gallbladder morphology and were assigned to node 5, one patient with Alagille syndrome and 2 patients with neonatal hepatitis. They had triangular cord thickness < 3.4 mm (range, 1.9–3.2 mm) (Fig. 3). Meanwhile, of the 39 BA patients with abnormal gallbladder morphology (node 5), 29 patients (74%) had triangular cord thickness > 3.4 mm.

Among the 7 BA patients with normal gallbladder morphology and triangular cord thickness > 3.4 mm in node 4, 5 patients were found to have the morphologic type IIIa—in which the hepatic ducts are obliterated and the cystic duct and CBD are patent—whereas the other 2 patients were found to have type IIIb, in which the CBD is fibrotic (Fig. 4) (19).

DISCUSSION

In this study, the diagnostic value of various US findings

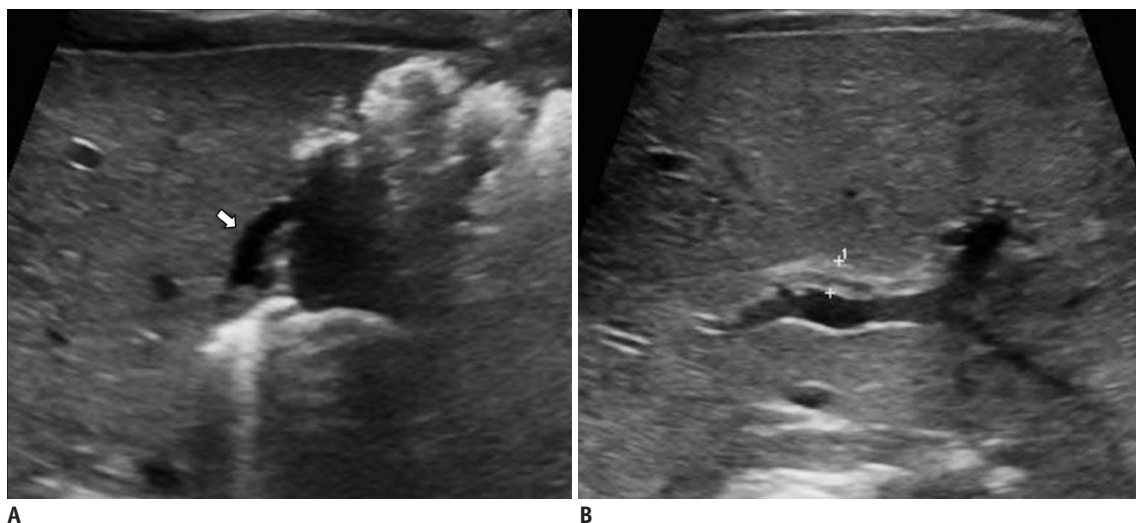


Fig. 2. 43-day-old female infant with BA. In conditional inference tree analysis, this patient was classified into node 5 owing to abnormal gallbladder morphology. **A.** Gallbladder (arrow) shows irregular wall and shape 11.9 mm in length. **B.** Triangular cord thickness is 4.1 mm. This is regarded as positive triangular cord sign. BA = biliary atresia

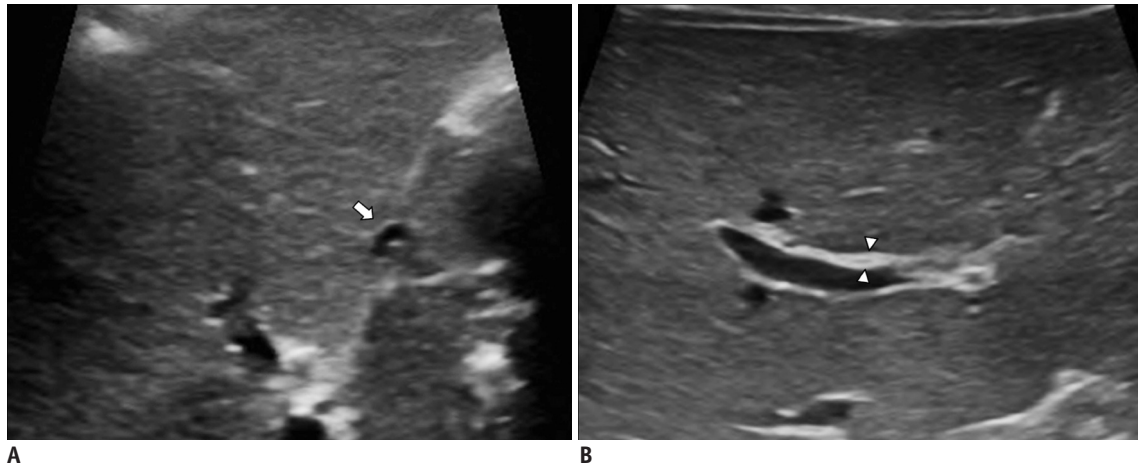


Fig. 3. 62-day-old female infant with neonatal hepatitis.

In conditional inference tree analysis, this patient was incorrectly classified into node 5 owing to abnormal gallbladder morphology. **A.** Gallbladder (arrow) has irregular contour with lack of complete echogenic mucosal lining. Gallbladder length is 3.1 mm. **B.** Triangular cord thickness (arrowheads) is 2.5 mm. This is regarded as negative triangular cord sign.

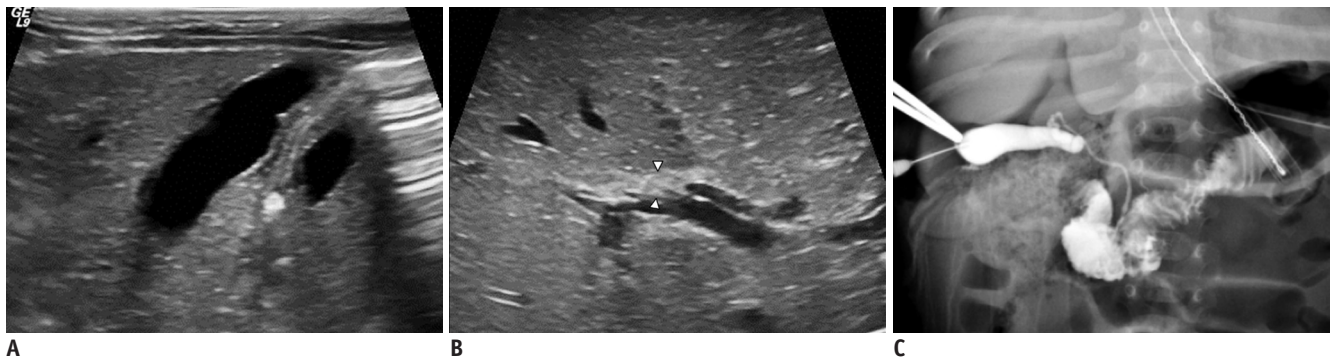


Fig. 4. 52-day-old male infant with BA.

In conditional inference tree analysis, this patient was classified into node 4 owing to normal gallbladder morphology and positive triangular cord sign (triangular cord thickness > 3.4 mm). **A.** Gallbladder has uniformly thin wall with smooth mucosal lining. Gallbladder length is 25.7 mm. **B.** Triangular cord thickness (arrowheads) is 4.7 mm. **C.** On intraoperative cholangiography, common bile duct and cystic duct are patent; however, common hepatic and intrahepatic bile ducts are not visualized. This patient is found to have Kasai type IIIa. BA = biliary atresia

was evaluated. Although many US features showed a significant association with BA in the univariate analysis, only 2 findings—abnormal gallbladder morphology and greater triangular cord thickness—were selected as independent predictors of BA in the multivariate analysis. Moreover, the conditional inference tree analysis selected these 2 findings as discriminators.

Similar to previous reports (6, 17, 18), our results showed that abnormal gallbladder morphology was the most significant predictor of BA in the multivariate and conditional inference tree analyses. Abnormal gallbladder morphology alone had been shown to have a sensitivity, specificity, and accuracy of 84.8% (39/46), 94.4% (51/54), and 90% (90/100), respectively, in the diagnosis of BA. However, abnormal gallbladder morphology may be seen in patients without BA but with severe intrahepatic cholestasis

(20, 21). In the present study, abnormal gallbladder morphology was seen in 1 patient who was diagnosed with Alagille syndrome and 2 patients with neonatal hepatitis. Moreover, 7 patients with BA (15%, type IIIa, n = 5; type IIIb, n = 2) had normal gallbladder morphology (node 4). A number of studies have reported that normal morphology and gallbladder length have been seen in patients with type IIIa, in which gallbladder and distal CBD appear to be less affected by the atretic process (10, 22–24), or even IIIb BA (22, 24, 25). BA is a dynamic process that leads to the obliteration of the bile ducts with progression of the US findings (3, 4, 6, 9, 24). Therefore, a normal gallbladder may be seen even in patients with type IIIb BA, in which the CBD is fibrotic.

The triangular cord sign has been reported to be a highly specific finding for the diagnosis of BA in many studies (4,

6-9, 12, 13, 22, 23, 25-28). However, variable sensitivities for this sign have been reported (range, 23–93%). A number of studies have used a triangular cord thickness of 4 mm as the objective criterion for triangular cord sign in BA (7, 12, 13, 28), whereas other studies have used 3 mm (22, 25). In the present study, 3.4 mm for the triangular cord thickness was selected as a cutoff value for the triangular cord sign in the conditional inference tree analysis. The positive triangular cord sign (triangular cord thickness > 3.4 mm) alone resulted in a sensitivity of 78.2% (36/46), a specificity of 100% (54/54), and a diagnostic accuracy of 90% (90/100). Lee et al. (7) proposed that identifying the triangular cord sign using US relies on the pattern and size of the fibrous ductal remnant in the porta hepatis and that false negative results can occur in BA cases with relatively thin fibrous masses in the porta hepatis. Other studies have mentioned that the triangular cord sign may be inconspicuous in the early stage of some BA cases and may evolve with age (4, 9, 23, 24, 28). Therefore, we concluded that the absence of the triangular cord sign cannot exclude the possibility of BA and that the presence of other predictive US findings—such as abnormal gallbladder morphology—should be more carefully evaluated.

Regarding visualization of the CBD, our data showed no statistical significance, even though Humphrey and Stringer (27) reported a high diagnostic value of CBD visibility. We believe that we found no significance because of the limited reliability of this finding in our study because no patients were sedated during their US examinations. Furthermore, as mentioned by Azuma et al. (11), subtype <a> (BA with a patent CBD) in the morphologic BA classification system (19) can result in a false-negative finding. In the present study, CBD was visible in 3 patients with BA (7%), and these infants were found at surgery to have fibrotic ducts without patent CBD. Therefore, we postulate that CBD can be visible on high-resolution US in subtype as well as in subtype <a>.

Hepatic subcapsular flow, which was not evaluated in the present study, has been reported to be highly sensitive for the diagnosis of BA (13, 14). Lee et al. (13) reported that hepatic subcapsular flow on color Doppler US images had sensitivity and specificity of 100% and 86%, respectively, and subcapsular telangiectasia was revealed in all patients with BA. Those authors postulated that hepatic arteriopathy in BA might be related to hepatic fibrosis, and this concept is supported by El-Guindi et al. (14); hepatic subcapsular flow had both sensitivity and specificity of 96.3% and grade of fibrosis in liver biopsies was significantly different

between the BA and non-BA groups. However, hepatic subcapsular flow was not assessed in most of our cases, for which US had been performed before this sign became generally known.

For the above-mentioned reasons, the diagnosis of BA cannot be made solely by a single US finding. In this context, we attempted to develop a decision-making tree model. The model had very high sensitivity (100%, 46 of 46) and acceptable specificity (94.4%, 51 of 54). We believe that the high sensitivity in this model is important because not missing patients with BA is more important considering poor prognosis associated with a delayed diagnosis.

As mentioned above, US is useful for excluding BA, but it is limited by the operator's experience. The feasibility of MR cholangiography has been studied for reliable diagnosis of BA. However, the diagnostic value of MR cholangiography for BA, in particular specificity, is still under debate (sensitivity, 90–100%; specificity, 36–96%; diagnostic accuracy, 71–98%) (29-31). We think that MR cholangiography can play a role in supplementary screening because of its high sensitivity when the utility of US is limited.

There were a number of limitations in the present study. First, the study was based on retrospective data collection. Second, gallbladder morphology was subjectively assessed; that is, the interpretation of the US findings might have depended on the operator's experience. Third, the small (submillimeters) sizes of the structures, such as the triangular cord thickness, hepatic artery, and CBD, could have resulted in measurement errors. Fourth, CBD detection had limited reliability based on the patients' cooperation because the infants were not sedated during the US examinations, as mentioned above. Fifth, another important sign of hepatic subcapsular flow was not evaluated in most of our cases because this sign had been reported only recently.

In conclusion, the present study revealed that abnormal gallbladder morphology and greater triangular cord thickness (> 3.4 mm) were the most significant predictors of BA on US. If patients show normal gallbladder morphology and triangular cord thickness ≤ 3.4 mm, the possibility of BA could be safely excluded. We suggest that gallbladder morphology should be evaluated first and then triangular cord thickness in cases with normal-looking gallbladders. Following the conditional inference tree model, 97 of the 100 patients were correctly classified into the BA or non-

BA groups. This decision tree could enable a more staged approach in clinical practice for the diagnosis of BA using US.

Supplementary Materials

The online-only Data Supplement is available with this article at <http://dx.doi.org/10.3348/kjr.2015.16.6.1364>.

REFERENCES

- Balistreri WF, Grand R, Hoofnagle JH, Suchy FJ, Ryckman FC, Perlmutter DH, et al. Biliary atresia: current concepts and research directions. Summary of a symposium. *Hepatology* 1996;23:1682-1692
- Valayer J. Conventional treatment of biliary atresia: long-term results. *J Pediatr Surg* 1996;31:1546-1551
- Ikeda S, Sera Y, Ohshiro H, Uchino S, Akizuki M, Kondo Y. Gallbladder contraction in biliary atresia: a pitfall of ultrasound diagnosis. *Pediatr Radiol* 1998;28:451-453
- Park WH, Choi SO, Lee HJ, Kim SP, Zeon SK, Lee SL. A new diagnostic approach to biliary atresia with emphasis on the ultrasonographic triangular cord sign: comparison of ultrasonography, hepatobiliary scintigraphy, and liver needle biopsy in the evaluation of infantile cholestasis. *J Pediatr Surg* 1997;32:1555-1559
- Nicotra JJ, Kramer SS, Bellah RD, Redd DC. Congenital and acquired biliary disorders in children. *Semin Roentgenol* 1997;32:215-227
- Visrutaratna P. Biliary atresia: making the diagnosis by the gallbladder ghost triad. *Pediatr Radiol* 2003;33:902; author reply 903
- Lee HJ, Lee SM, Park WH, Choi SO. Objective criteria of triangular cord sign in biliary atresia on US scans. *Radiology* 2003;229:395-400
- Park WH, Choi SO, Lee HJ. Technical innovation for noninvasive and early diagnosis of biliary atresia: the ultrasonographic "triangular cord" sign. *J Hepatobiliary Pancreat Surg* 2001;8:337-341
- Choi SO, Park WH, Lee HJ, Woo SK. 'Triangular cord': a sonographic finding applicable in the diagnosis of biliary atresia. *J Pediatr Surg* 1996;31:363-366
- Weinberger E, Blumhagen JD, Odell JM. Gallbladder contraction in biliary atresia. *AJR Am J Roentgenol* 1987;149:401-402
- Azuma T, Nakamura T, Nakahira M, Harumoto K, Nakaoka T, Moriuchi T. Pre-operative ultrasonographic diagnosis of biliary atresia--with reference to the presence or absence of the extrahepatic bile duct. *Pediatr Surg Int* 2003;19:475-477
- Kim WS, Cheon JE, Youn BJ, Yoo SY, Kim WY, Kim IO, et al. Hepatic arterial diameter measured with US: adjunct for US diagnosis of biliary atresia. *Radiology* 2007;245:549-555
- Lee MS, Kim MJ, Lee MJ, Yoon CS, Han SJ, Oh JT, et al. Biliary atresia: color doppler US findings in neonates and infants. *Radiology* 2009;252:282-289
- El-Guindi MA, Sira MM, Konsowa HA, El-Abd OL, Salem TA. Value of hepatic subcapsular flow by color Doppler ultrasonography in the diagnosis of biliary atresia. *J Gastroenterol Hepatol* 2013;28:867-872
- Hothorn T, Hornik K, Zeileis A. Unbiased recursive partitioning: a conditional inference framework. *J Comput Graph Stat* 2006;15:651-674
- Zhou LY, Wang W, Shan QY, Liu BX, Zheng YL, Xu ZF, et al. Optimizing the US diagnosis of biliary atresia with a modified triangular cord thickness and gallbladder classification. *Radiology* 2015;277:181-191
- Farrant P, Meire HB, Mieli-Vergani G. Ultrasound features of the gall bladder in infants presenting with conjugated hyperbilirubinaemia. *Br J Radiol* 2000;73:1154-1158
- Farrant P, Meire HB, Mieli-Vergani G. Improved diagnosis of extrahepatic biliary atresia by high frequency ultrasound of the gall bladder. *Br J Radiol* 2001;74:952-954
- Ohi R, Masaki N. *The jaundiced infant: biliary atresia and other obstructions*. In: O'Neill JA Jr, Rowe MI, Grosfeld JL, Fonkalsrud EW, Coran AG, eds. *Pediatric surgery*. Philadelphia: Mosby Elsevier, 1998:1465-1481
- Burton EM, Babcock DS, Heubi JE, Gelfand MJ. Neonatal jaundice: clinical and ultrasonographic findings. *South Med J* 1990;83:294-302
- Kirks DR, Coleman RE, Filston HC, Rosenberg ER, Merten DF. An imaging approach to persistent neonatal jaundice. *AJR Am J Roentgenol* 1984;142:461-465
- Takamizawa S, Zaima A, Muraji T, Kanegawa K, Akasaka Y, Satoh S, et al. Can biliary atresia be diagnosed by ultrasonography alone? *J Pediatr Surg* 2007;42:2093-2096
- Park WH, Choi SO, Lee HJ. The ultrasonographic 'triangular cord' coupled with gallbladder images in the diagnostic prediction of biliary atresia from infantile intrahepatic cholestasis. *J Pediatr Surg* 1999;34:1706-1710
- Lee SY, Kim GC, Choe BH, Ryeom HK, Jang YJ, Kim HJ, et al. Efficacy of US-guided percutaneous cholecystocholangiography for the early exclusion and type determination of biliary atresia. *Radiology* 2011;261:916-922
- Kanegawa K, Akasaka Y, Kitamura E, Nishiyama S, Muraji T, Nishijima E, et al. Sonographic diagnosis of biliary atresia in pediatric patients using the "triangular cord" sign versus gallbladder length and contraction. *AJR Am J Roentgenol* 2003;181:1387-1390
- Tan Kendrick AP, Phua KB, Ooi BC, Subramaniam R, Tan CE, Goh AS. Making the diagnosis of biliary atresia using the triangular cord sign and gallbladder length. *Pediatr Radiol* 2000;30:69-73
- Humphrey TM, Stringer MD. Biliary atresia: US diagnosis. *Radiology* 2007;244:845-851
- Mittal V, Saxena AK, Sodhi KS, Thapa BR, Rao KL, Das A, et al. Role of abdominal sonography in the preoperative diagnosis of extrahepatic biliary atresia in infants younger than 90 days. *AJR Am J Roentgenol* 2011;196:W438-W445
- Han SJ, Kim MJ, Han A, Chung KS, Yoon CS, Kim D, et al.

- Magnetic resonance cholangiography for the diagnosis of biliary atresia. *J Pediatr Surg* 2002;37:599-604
30. Norton KI, Glass RB, Kogan D, Lee JS, Emre S, Shneider BL. MR cholangiography in the evaluation of neonatal cholestasis: initial results. *Radiology* 2002;222:687-691
31. Liu B, Cai J, Xu Y, Peng X, Zheng H, Huang K, et al. Three-dimensional magnetic resonance cholangiopancreatography for the diagnosis of biliary atresia in infants and neonates. *PLoS One* 2014;9:e88268